Absorber characterization
COMPASS thesis

Armando Brandonisio

April 25, 2016

Contents

Chapter 1

Absorber characterization

We investigated luminescence and scintillation properties of the $Gd_3Al_2Ga_3O_{12}:Ce$ (GAGG) produced by *Furukawa* company. The GAGG crystal has the highest light yield among oxide crystal at room temperature [1] and fast decay time for the detection of radioactivity and in nuclear and particle physics experiments.
A list of the most important parameters for GAGG is reported in Table 1.1.

Some fundamental features of this crystal are that it has no intrinsic radioactivity and it is a non-hygroscopic material. This allows a better usage for experimentation with low risk of contamination from ambient.

The measurements have been carried out by illuminating the scintillation rod with a X-ray beam.
*Si*PM and electronic chain parameters was varied measuring the relative position of the photo-peak in the spectrum produced by the scintillator.

Density $[g/cm^3]$	Light yield [photon/MeV]	Decay time [ns]	Peak emission [nm]	Energy resolution [% @662 keV]	Hygroscopicity
6.63	57000	88 (91%) 258 (9%)	520	5.2	No

Table 1.1: Physical and scintillation properties of GAGG

1.1 Experimental set-up

Laboratory measurements have been carried out using a single rod made of GAGG produced by *Furukawa* company.
The rod has a square-base parallelepipoidale shape with a height of 30mm and a side of 3mm , thus their dimension results 2/3 lower to the one expected for the polarimeter bars ($\sim 10mm$).
To minimize the loss of photons during scintillation, the bar was *wrapped* with Teflon Fig 1.1, that has a high r~~eflection~~ coefficient for small incident angles.

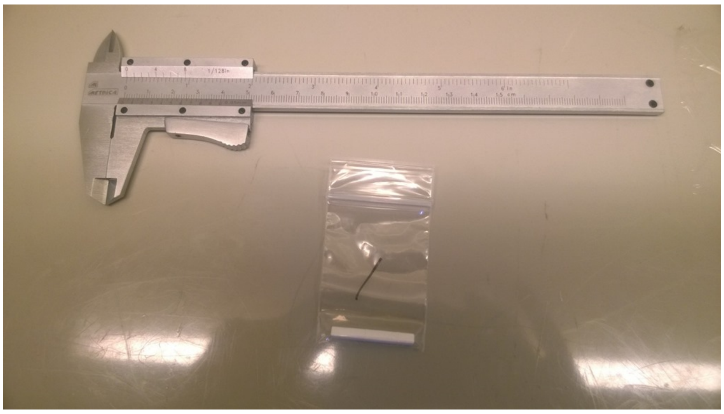

Figure 1.1: Scintillation rod made of GAGG wrapped with teflon

The rod has been placed over a single SiPM, models LCT4/9 and LCT5/1 produced by the Hamamatsu company.
Properties, CAD scheme and microscopic details of this SiPM are reported in Tab 1.2, Fig 1.2 and Fig 1.3 respectively.

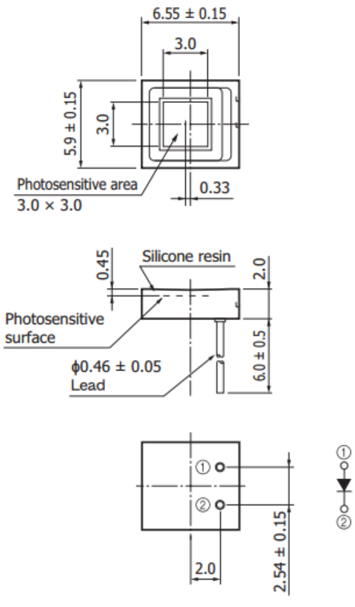

Figure 1.2: CAD scheme for LCT4/9 and LCT5/1

LCT4/9	
Cell pitch	$75\mu m$
Device size	$3 \times 3 mm^2$
Microcells	1600
Surface coating	Silicone resin
Fill-factor	73%
Breakdown[1]	51.10 V

LCT5/1	
Cell pitch	$50\mu m$
Device size	$3 \times 3 mm^2$
Microcells	3600
Surface coating	Silicone resin
Fill-factor	74%
Breakdown[2]	52.5 V

Table 1.2: Main physical features of LCT/9 and LCT5/1

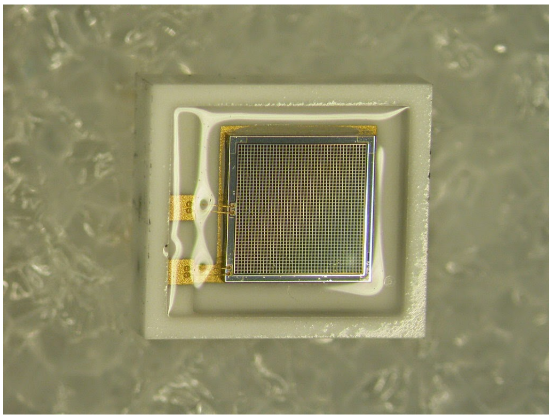

Figure 1.3: Image of LCT4/9 taken through a microscope.

This set of MPPCs produced by Hamamatsu, have an included proprietary circuit board with power supply for a direct hardware control from PC via USB connection (see Fig 1.4).
The C12332 is a simple evaluation starter kit for non-cooled MPPC. MPPC evaluation is possible by mounting an MPPC in the socket of the sensor circuit board. The power supply circuit board is equipped with the C11204-01, a high-accuracy, high-voltage power supply that provides the operating voltage from MPPC. It operates just by connecting to an extenal power supply ($\pm 5V$). It is also equipped with a USB interface that can be used to set the operating voltage and temperature compensation coefficient from a PC running the supplied sample software.
We used the power supply circuit board with serial number C12332 with nominal gain of 21 for LCT4/9.

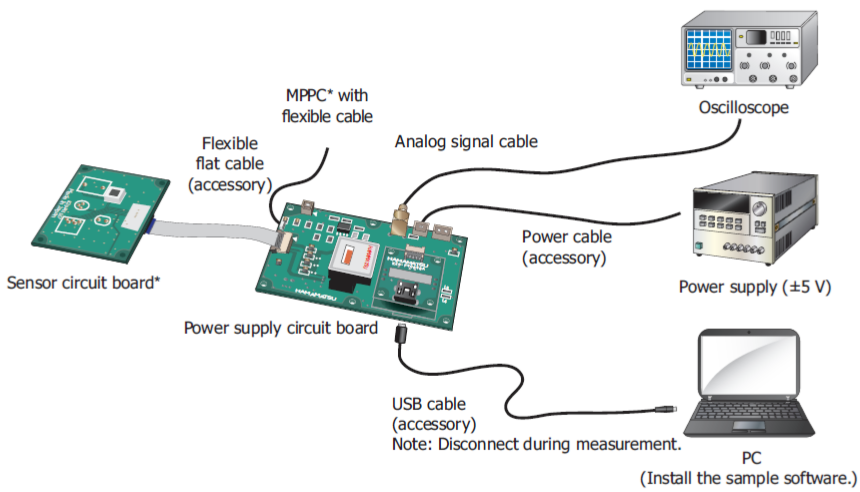

Figure 1.4: Connection example

Sensor circuit and power supply board have been both fixed on an aluminum support covered by black duct tape (Fig 1.5).

Figure 1.5: Circuit and sensor boards on support

The GAGG rod has been placed over a single SiPM. The extremity of the rod in contact with the SiPM window entrance has been covered with optical grease in order to improve the transmission of optical photons to the microcells.
A dedicated support has been projected and realized specifically for this experiment in order to hold the rod under study and to guarantee its contact with the SiPM.
The project drawing is reported in Fig 1.6 and the principal components legend below:

- (1) Aluminum support
- (2) secondary mobile support for power supply circuit board
- (4) dark box
- (6-7) support columns
- (8) support for rod-stops
- (9) rod stops
- (11) circular support for x-ray sources

The produced support inserted in the experimental set-up is shown in Fig 1.7.

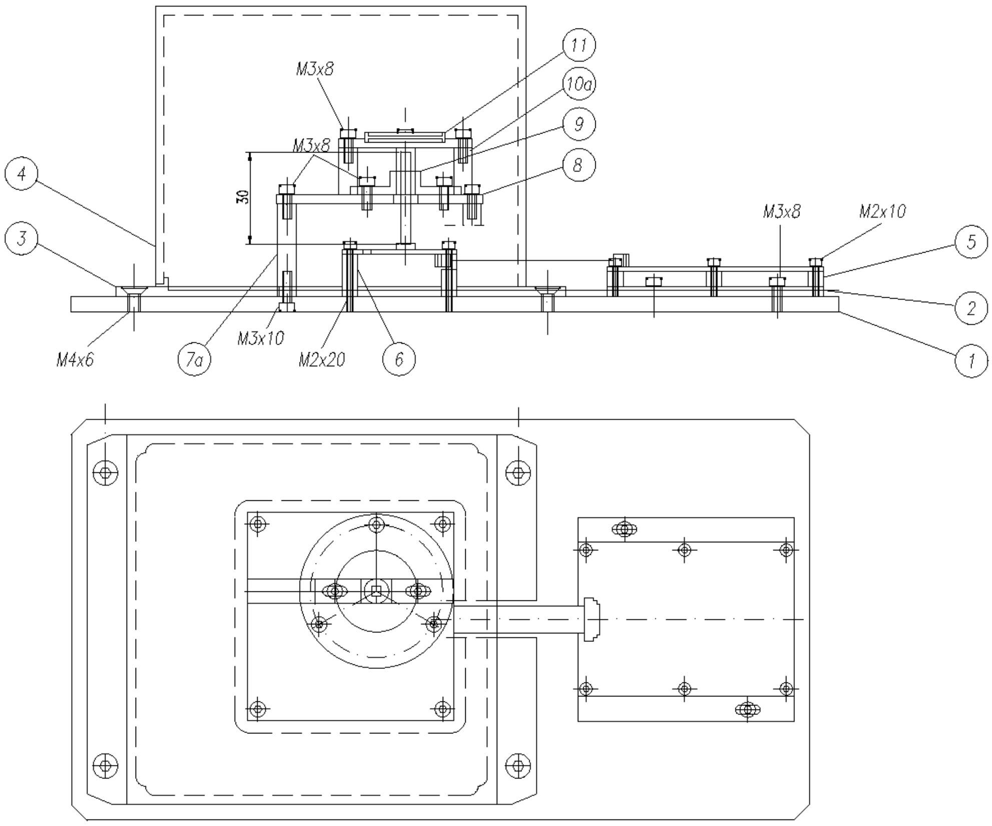

Figure 1.6: Front and side projection of entire setup.

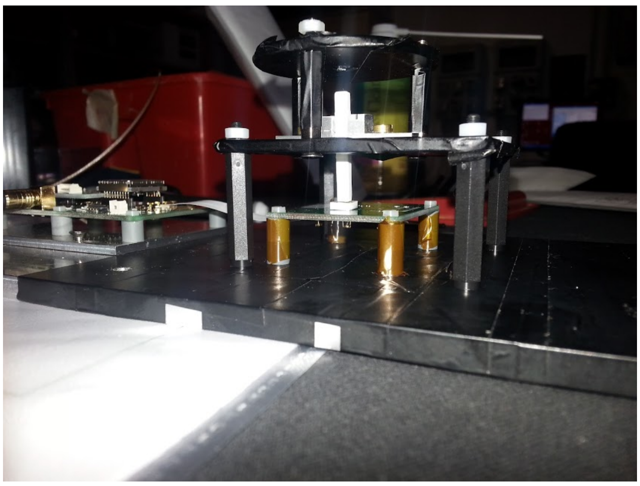

Figure 1.7: Built setup

Sources of ^{241}Am, ^{109}Cd, ^{133}Ba, ^{55}Fe, ^{137}Cs have been used to illuminate the rod, placed at a distance of about 5mm from the rod top, put on a circular aluminum support designed for the used radioactive sources. The source has a diameter of 1mm. It's flux ~~hasn't~~ been collimated.
The alignment of the source along Z-direction has been carried out optically because the diameter of the beam spot was larger than the rod one, and therefore a rough alignment was sufficient.
The SiPM signal was read and processed by electronic chain whose diagram is reported in Fig 1.8. Power supply circuit board permitted to vary the operative voltage applied to the SiPM through USB connection and thus the SiPM internal gain.
The signal from SiPM was processed by a pre-amplifier welded on Hamamatsu circuit board and an amplifier ORTEC 450 *Research Amplifier*, and then digitized by a Multi-Channel Analyzer (MCA) Amptek 8000A, which splits signal into 1024 digital channels in a dynamic range of 0-5V or 0-10V.
The SiPM is very sensitive to visible light, therefore dark conditions are needed to perform the measurements. The dark conditions were assured by a *dark box* ((4) in Fig 1.6), a carton and a black cloth placed over the set-up.

ELECTRONIC CHAIN

Figure 1.8: Sketch scheme of the electronic chain employed in the measurements to read and store SiPM signals

1.2 Definition of the operative range

1.2.1 Set-up parameters

Some preliminary operations must be performed before starting the measurement process. In particular, the parameters of the electronic chain must be set to proper values, the digital channels of the MCA must be converted into charge values through a calibration and the experimental conditions must be analyzed.

The gains of the used SiPM and amplifier can be varied. It has been necessary to properly set these parameters in order to generate a signal within a range suitable to the MCA input dynamics.
During the adjusting process, the gains were changed until the whole signal from the SiPM has been included in the spectrum collected by the MCA. An intense light source was necessary to guarantee a high measurement rate in order to collect a suitable number of events in a short time and to dominate dark current.
We know that our GAGG rod has a light yield of $\sim$ 60 photons/keV, and ^{241}Am source ~~has been chosen as relatively intense~~.

Here the instruments limitations:

- Hamamatsu datasheets says that we have a linearity of signal when we illuminate at the same time a number $< 40\% - 50\%$ of MPPC pixels.
- MPPC signals are very fast ($< 100ns$) and very frequents, but MCA accepts a minimum shaping time of $250ns$ with a 'first peak detection'.

In order to prevent saturations or non-linearity in the final spectrum, we chose set-up parameters so that ^{241}Am photo-peak @ $59.5keV$ was placed in the middle of MCA dynamic range.
Gain and integration time of ORTEC450 and *operative tension* (V_{op}) of SiPMs have been changed to optimize quality of spectrum.

1.2.2 Energy range

Qui devo aggiungere l'efficienza dei SiPM + GAGG
To define an energy range of measurement system we needed to know maximum efficiency interval for scintillator rod, SiPMs and both. Detector efficiency, as function of energy, is defined by:

$$\epsilon(E) = T(E) \cdot A(E) \tag{1.1}$$

where T(E) and A(E) are respectively (1.2) transparency (1.3) and absorption with respect to energy radiation.

$$T(E) = e^{-\rho\delta\sigma(E)} \tag{1.2}$$

$$A(E) = 1 - e^{-\rho\delta\sigma(E)} \tag{1.3}$$

ρ is the material density, δ the thickness and $\sigma(E)$ the cross section sums for coherent/incoherent Compton scattering and photoelectric effect as a function

of energy.
We know all GAGG properties (Tab 1.1) and cross section values with respect to energy[3]. Results value in Fig 1.9.

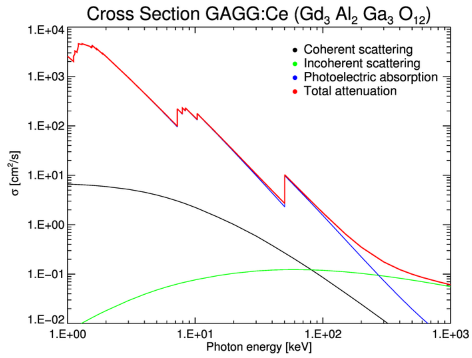

Figure 1.9: Mass attenuation coefficients for the GAGG crystal

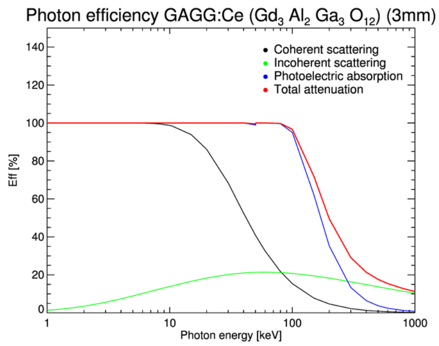

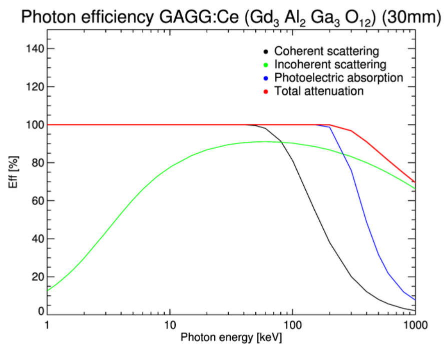

Figure 1.10: Total GAGG efficiency for a thickness of 3mm (left) and 30mm (right)

[3]Data from: XCOM: Photon Cross Sections Database (http://www.nist.gov/pml/data/xcom/)

1.3 Circuit calibration with X-ray sources

A calibration of the electronic chain has been performed in order to convert the digital channels of the MCA output spectra in charge values.
Signals with similar amplitude, rise time and fall time of SiPM was produced by a pulse generator (BNC BL-2).
The exact values of applied voltages have been measured through an oscilloscope connected to circuit. At the same time, the channel number of the peak produced by the signal in the MCA spectrum was stored and associated with the applied voltage.
This operation has been repeated for different V_{op} (Fig 1.11).

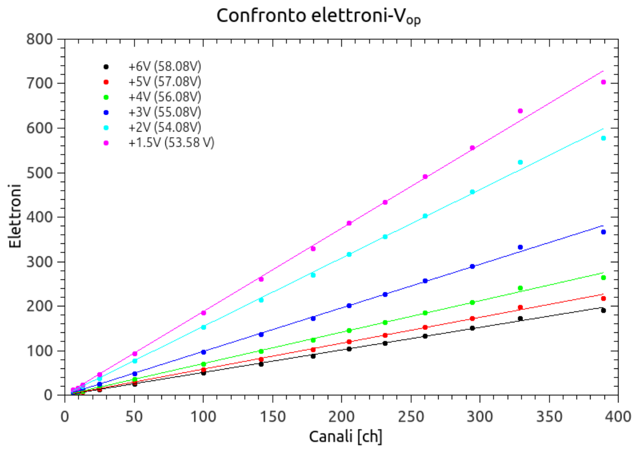

Figure 1.11: Linear calibration function used to convert the measured digital channels into charge values for LCT5/1.

Furthermore ~~an energy calibration was~~ performed with radioactive sources ~~cited~~ in section 1.1 (Fig 1.14).
Gaussian model was selected to fit sources photo-peaks. In order to improve fit, we studied a model that explain photopeak asymmetries for ^{109}Cd and ^{133}Ba (Fig 1.12).

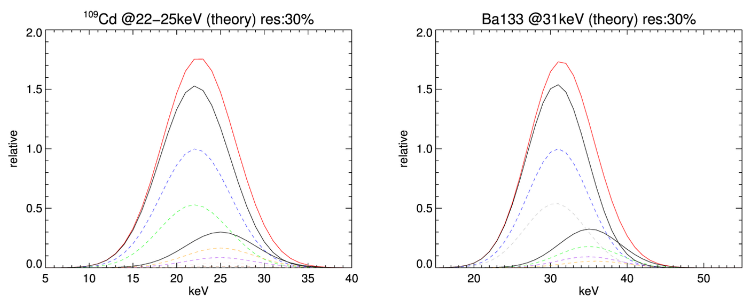

Figure 1.12: Theoretical model that assumes laboratory probability of each convoluted line for a resolution of 30%. Data from XCOM.

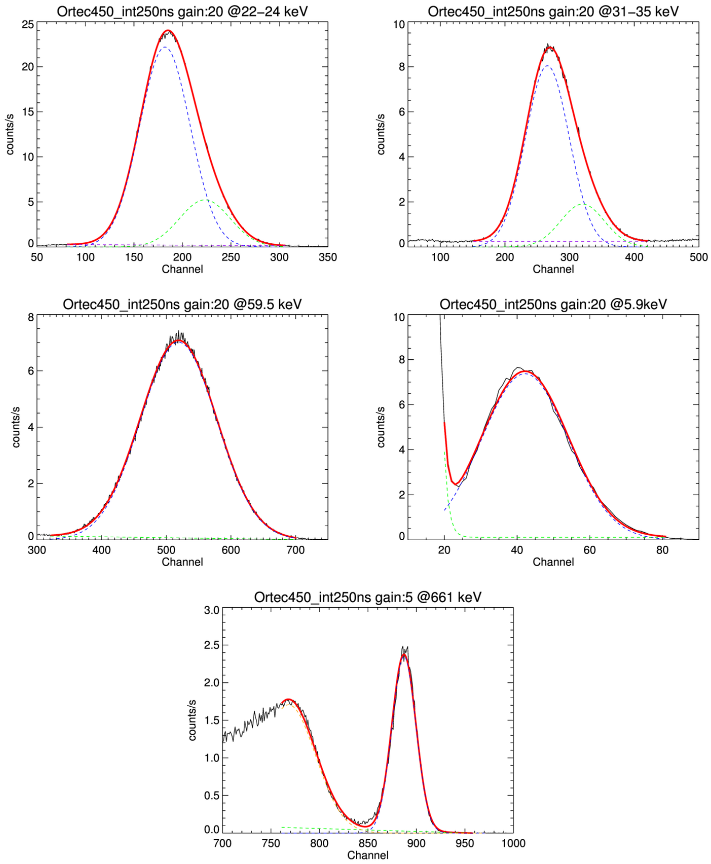

Figure 1.13: To left to right respectively: ^{109}Cd @ 22keV, ^{133}Ba @ 31keV, ^{241}Am @ 59.5keV, ^{55}Fe @ 5.9 kev, ^{137}Cs @ 661 keV

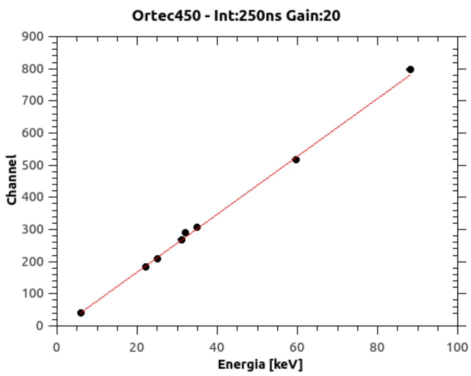

Figure 1.14: Linear energy calibration in the range of 0-90KeV for LCT4/9.

We also detected non-linearity for high energies values as expected (Fig 1.15).

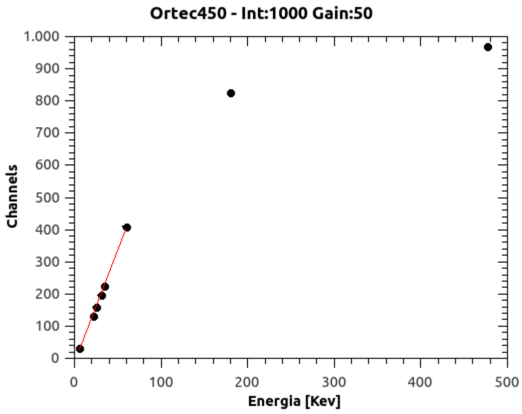

Figure 1.15: Non-linearity detection at high energies with LCT4/9.

1.3.1 Dark/Background noise

Background noise spectra (Fig 1.16) are fundamental informations to select best configuration for acquiring data.
A study of *dark* counts has been performed to understand behavior of SiPM as V_{op} changes.

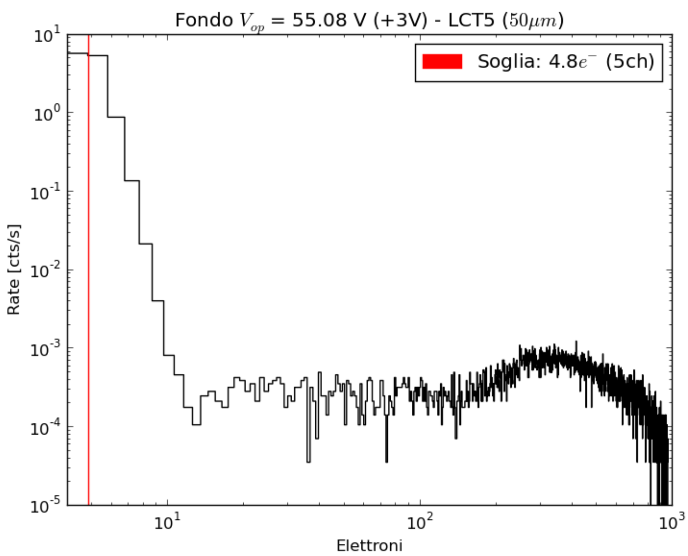

Figure 1.16: Background noise acquisition with LCT5/1 ($V_{op} = +3V$)+ GAGG.

~~Ambient noise~~ is negligible with respect to sources rate. At low charge collection dark current dominates.
An exponential curve was chosen to fit dark noise (Fig 1.17).

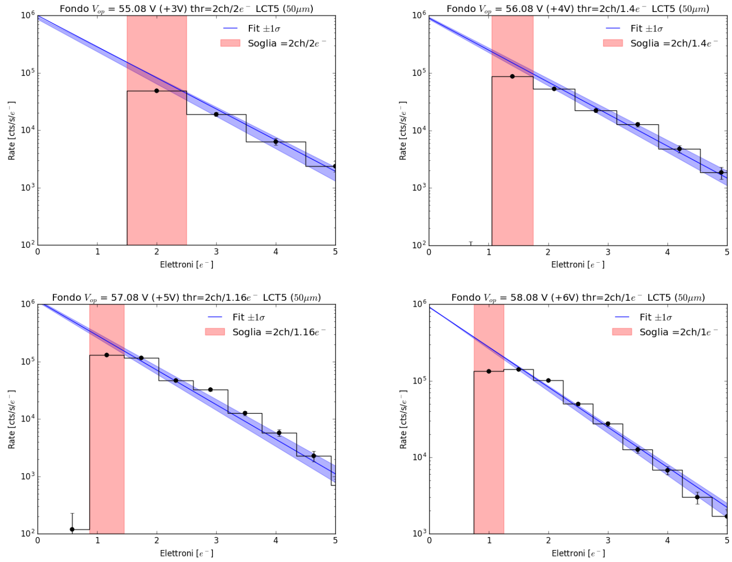

Figure 1.17: Dark rate study for LCT5/1+ GAGG

1.4 Energy resolution measurement

Fitted sources photopeaks of section 1.3 has been analyzed to extrapolate energy resolution as a function of V_{op}.
We note that dark rate increases with the increase of V_{op} but resolution seems to be better (decreases) with V_{op}.
Left plot of Fig 1.18 (^{55}Fe @ 5.9 kev), has an irregular distribution with respect to ^{241}Am case, due to nearness of dark noise that affects error of photopeak position and width.

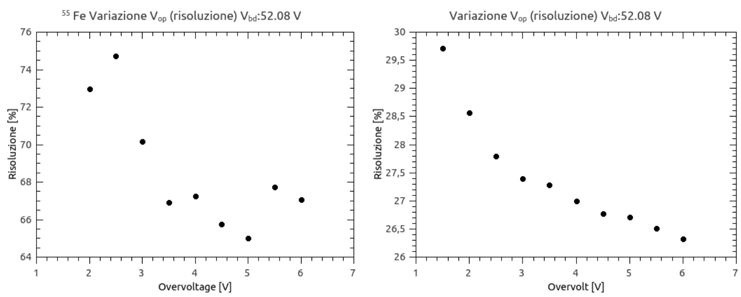

Figure 1.18: Resolution for ^{55}Fe peak (left) and (^{241}Am) peak as function of V_{op}.

Bibliography

[1] Hye-Lim Kim et al. Journal of Ceramic Processing Research. Vol. 16, No. 1, pp. 124-128, 2015